

SMALL HORIZONTAL AXIS WIND TURBINE: ANALYTICAL BLADE DESIGN AND COMPARISON WITH RANS-PREDICTED FLOW FIELD AND PERFORMANCE DATA

T. Gerhard - T. H. Carolus

University of Siegen, Institut für Fluid- und Thermodynamik, 57068 Siegen, Germany
tom.gerhard@uni-siegen.de, thomas.carolus@uni-siegen.de

ABSTRACT

An analytical method for designing axial wind turbine blades is described. It is based on the classical blade element momentum (BEM) model, but formulated in terms of velocity triangles, Euler's turbine equation, and the vector mean velocity from in- to outlet in the rotating frame of reference. Airfoil lift and drag are determined via XFOIL. A small axial wind turbine is designed by means of this analytical tool. Then a 3D RANS simulation at design operation is performed. For turbulence modeling we use the standard shear stress transport, and, alternatively, a laminar/turbulent transition model. Local values such as the induction factors, the pressure distributions and integral performance data are compared. Although the blade boundary layer is basically transitional, the accuracy of the numerical results utilizing the laminar/turbulent transition model and the shear stress transport model is similar as compared to the analytical design target.

NOMENCLATURE

A	area (m ²)	p	static pressure (Pa)	Subscripts	
C_P	power coefficient (-)	r	radius (m)	0	position far upstream
D	drag force (N)	t	blade spacing (m)	1	position before rotor
F_{ax}	axial force (N)	u	circumferential velocity (m/s)	2	position after rotor
F_u	tangential force (N)	w	relative velocity (m/s)	3	position far downstream
L	lift force (N)	z	number of blades (-)	∞	position in rotor plane
P	power (W)	α	angle of attack (°)	BE	blade element
R	radius (m)	β	flow angle (°)	D	diameter
Re	Reynolds number (-)	γ	intermittency factor (-)	a	ambient
a	axial induction factor (-)	ε	drag/lift ratio (-)	ave	average
a'	tangential induction factor (-)	η	efficiency (-)	$drag$	profile drag
c_F	friction coefficient (-)	λ	tip speed ratio (-)	dyn	dynamic
c_L	lift coefficient (-)	ν	kin. viscosity (m ² /s)	hub	at hub
c_m	absolute axial flow (m/s)	ρ	density (kg/m ³)	m	meridional (axial)
c_p	pressure coefficient (-)	σ	solidity (-)	r	radial position
c_u	absolute circumferential velocity (m/s)	τ	shear stress (N/m ²)	tip	blade tip
l	chord length (m)			u	circumferential
\dot{m}	mass flow rate (kg/s)				

INTRODUCTION

The paper deals with the aerodynamic performance prediction of horizontal axis wind turbines employing a blade element momentum (BEM) based analytical method and a numerical flow simulation. State-of-the-art performance prediction tools are often based on semi-analytical models, incorporating some form of BEM analysis, extended airfoil polar curves and other empirical assumptions for off-design operation (see e.g. Hansen in Brouchaert, 2007 or Hansen, 2009). In

principle, computational fluid dynamics (CFD) methods can yield the fundamental performance of a wind turbine without empirical assumptions. They also have the potential to be linked to structural and aeroacoustic computational tools. Inherent difficulties, however, are (i) the large computational domain required to capture all effects of the unbounded ambient flow field on the rotor and (ii) the fact that the near-blade flow field is transitional from laminar to turbulent.

Almost any performance prediction tool needs the geometry of the wind turbine as an input. BEM-based design tools are most common for blade design. In many of these methods a blade is considered as an isolated wing subject to an approaching flow under a given angle of attack (see e.g. Spera, 1998, Gasch and Tewe, 2002, Burton et al., 2008, Manwell et al., 2009). By contrast, designers of other low solidity axial turbomachinery (such as low pressure fans) often start with a cascade of blades and velocity triangles at the rotor's entrance and exit planes (see e.g. Carolus and Starzmann, 2011). Then the meridional component of the absolute velocity is linked to the volume flow rate through the rotor and the tangential component of the exit flow to the work done by the rotor (via Euler's equation of turbomachinery). To be consistent the relevant velocity for lift and drag of the wing type blade flow approaching the rotor must be replaced by the vector mean of the relative flow at rotor entrance and exit plane. Probably Hütter, 1942, was among the first applying this idea to the design of wind turbines. The benefit of this formulation is that design quantities can readily be compared with circumferentially averaged data up and downstream of the rotor from CFD.

A first objective of this study is the formulation of the standard analytical blade design method in terms of cascade inlet and outlet velocity triangles, integrating XFOIL (Drela, 1989) as airfoil performance predictor. With that, a 3 m rotor diameter axial wind turbine with low Reynolds number Somers airfoil sections (Somers, 2005) is designed. A second objective is the evaluation and assessment of the flow and power yield of this wind turbine operating at its design point employing a steady, incompressible, three-dimensional, Reynolds-averaged Navier-Stokes (RANS) simulation. Two different turbulence models selected within the RANS simulations are compared: (i) a standard turbulence model without transition and (ii) a laminar/turbulent transition model.

ANALYTICAL BLADE DESIGN METHOD

Fig. 1 shows a wind turbine with a boundary stream tube. The free stream wind speed far upstream of the rotor is c_0 . It eventually is decelerated to c_3 far downstream. At any coaxial strip at a given radius containing a number of blade elements one can draw the velocity triangles at the rotor entrance and exit plane, Fig. 2. Ideally, the absolute flow enters the rotor perpendicular with the velocity $c_1 = c_{m1}$, i.e. without swirl and leaves it with the velocity of the deflected flow c_2 . Since the axial extension of the rotor is small, we assume the meridional (i.e. axial through flow) velocity at rotor entrance and exit plane being equal, $c_{m1} = c_{m2}$. As usual, an axial induction factor a is defined such that

$$c_{m1} = c_{m2} = c_m = (1 - a)c_0 \text{ and } c_{m3} = (1 - 2a)c_0. \quad (1a, b)$$

Moreover, c_2 has the tangential component c_{u2} (i.e. the swirl) which is the key quantity for work extracted from the flow by the blades. As usual, a tangential induction factor a' is defined such that

$$c_{u2} = -2a'u. \quad (2)$$

The mass flow through the bladed annulus is

$$\delta\dot{m} = \rho c_m 2\pi r \delta r = \rho(1 - a)c_0 2\pi r \delta r. \quad (3)$$

From axial momentum conservation on the complete coaxial strip in the stream tube one obtains the axial force on the strip as

$$\delta F_{ax} = (c_0 - c_{m3}) \delta\dot{m} = a(1 - a)c_0^2 \rho 4\pi r \delta r. \quad (4)$$

Alternatively, the axial thrust force is also

$$\delta F_{ax} = (p_2 - p_1) \delta A \quad (5)$$

where p_1 and p_2 are the static pressure up- and downstream of the bladed annulus.

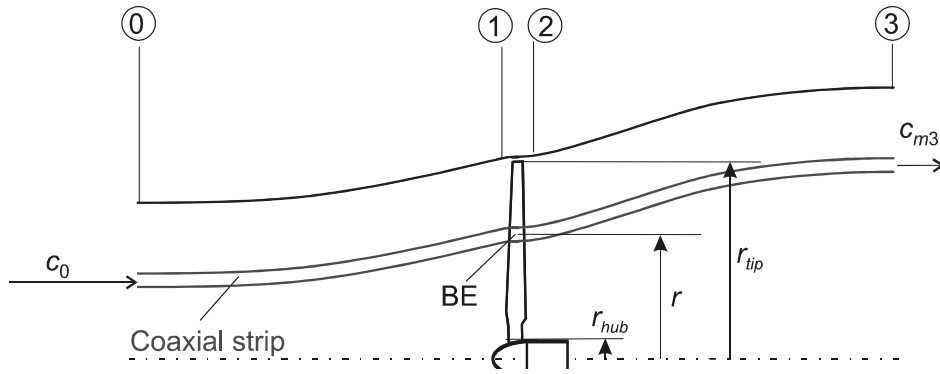


Fig. 1: Wind turbine rotor in boundary stream tube

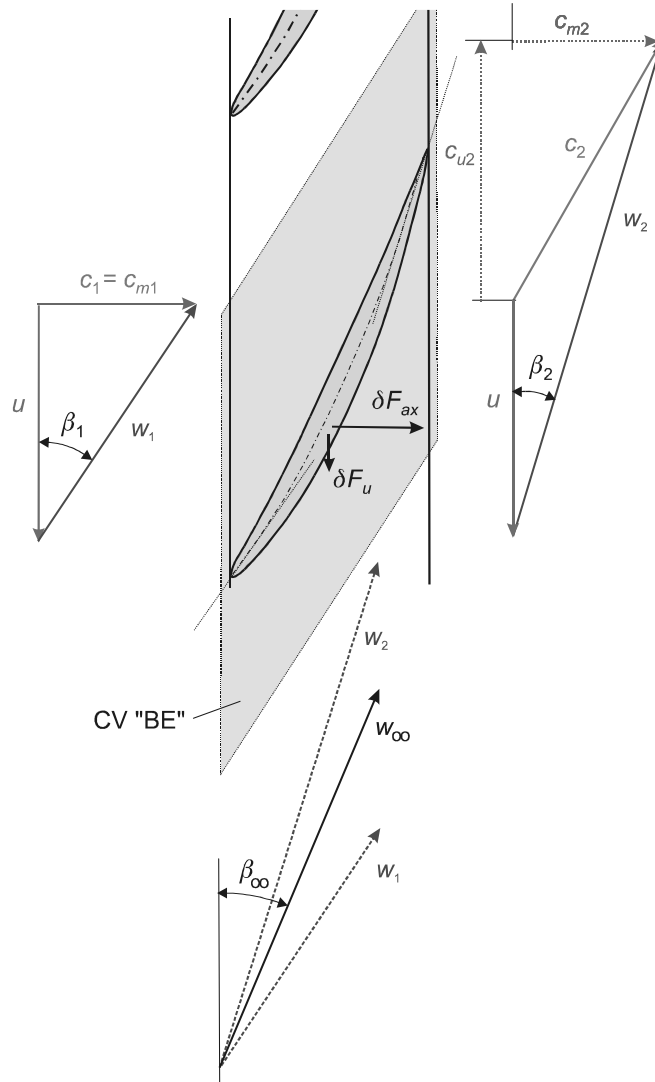


Fig. 2: Wind turbine rotor: Entrance and exit plane velocity triangle and vector mean relative flow velocity w_∞

Employing Euler's equation of turbomachinery in the form

$$p_2 - p_1 = \frac{\rho}{2} (w_1^2 - w_2^2), \quad (6)$$

one obtains after some steps

$$\delta F_{ax} = \rho u^2 a' (1 + a') 4\pi r \delta r. \quad (7)$$

w_1 and w_2 are the flow velocities in the relative frame of reference. Eliminating δF_{ax} from eqs. (5) and (7) and introducing the tip-speed ratio and the local-speed ratio

$$\lambda = \frac{u_a}{c_0}, \quad \lambda_r = \frac{u}{c_0} \equiv \frac{r}{r_{tip}} \lambda \quad (8a, b)$$

we end up with a first equation for the unknown variables a and a'

$$a' = -\frac{1}{2} + \sqrt{\frac{1}{4} + \frac{a(1-a)}{\lambda_r^2}} = f(\lambda_r). \quad (9)$$

Again, according to Eulers's equation of turbomachinery, the power due to all blade elements in the coaxial strip is

$$\delta P_{BE} = u c_{u2} \delta \dot{m} = \rho u^2 a' (1-a) c_0 4\pi r \delta r. \quad (10)$$

The power provided by the wind

$$\delta P_{wind} = \frac{\rho}{2} c_0^3 2\pi r \delta r \quad (11)$$

serves to define a strip power coefficient in the usual way

$$C_{P, BE} \equiv \frac{\delta P_{BE}}{\delta P_{wind}} = 4a'(1-a)\lambda_r^2 = f(\lambda_r). \quad (12)$$

This is a second equation for the unknown variables a and a' . The strategy now is: For a set of local-speed ratios λ_r find a and a' from eqs. (9) and (12) which yield the *maximum* value of $C_{P, BE}$. A closed solution is difficult, but a simple iteration is rather straight forward. Eventually, we arrive at the known Glauert/Schmitz graph in Fig. 3 as published e.g. by Gasch and Twele (2002).

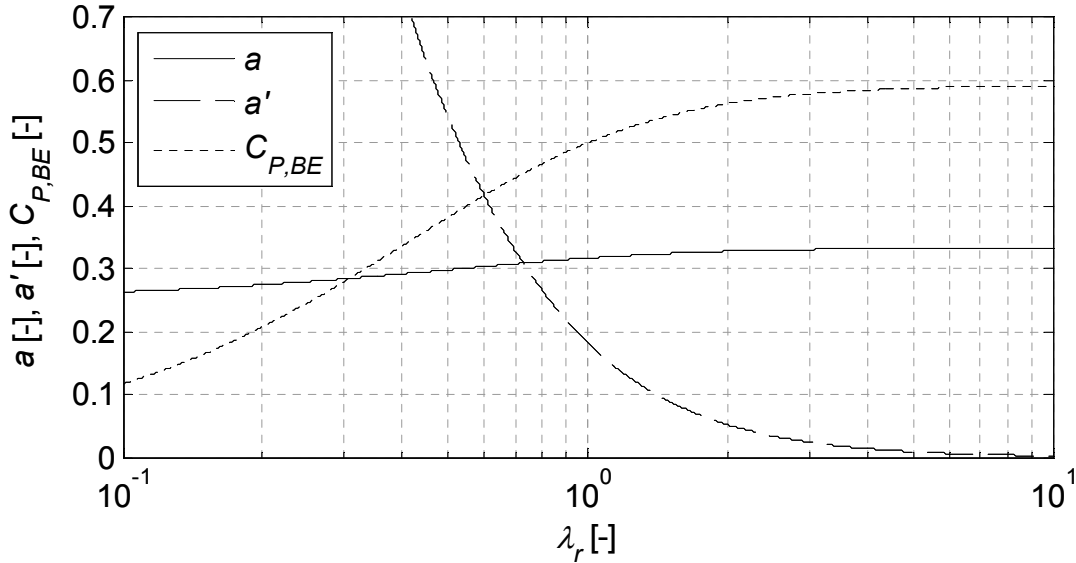


Fig. 3: Induction factors and strip power coefficient for maximum power (so called Glauert/Schmitz graph)

For a given lift and drag of a selected airfoil we now seek the solidity of the blade cascade, i.e. the ratio of blade element chord length to the circumferential spacing of the blades. Referring to Fig. 2, from angular momentum conservation the circumferential force on a blade element becomes

$$\delta F_u = c_{u2} \rho c_m t \delta r. \quad (13)$$

Introducing the vector mean velocity (Fig. 2)

$$\vec{w}_\infty \equiv \frac{1}{2} (\vec{w}_1 + \vec{w}_2) \quad (14)$$

we obtain

$$w_\infty = c_0(1-a)\sqrt{\left[\frac{(1+a')}{(1-a)}\right]^2 \lambda_r^2 + 1} \quad (15)$$

and

$$\beta_\infty = \arctan\left(\frac{1-a}{1+a'} \frac{1}{\lambda_r}\right). \quad (16)$$

Hence, from Fig. 4, the circumferential force on a blade element in terms of lift c_L and drag-lift ratio ε of the airfoil section becomes

$$\delta F_u = \sin(\beta_\infty - \varepsilon) c_L \rho \frac{w_\infty^2}{2} l \delta r. \quad (17)$$

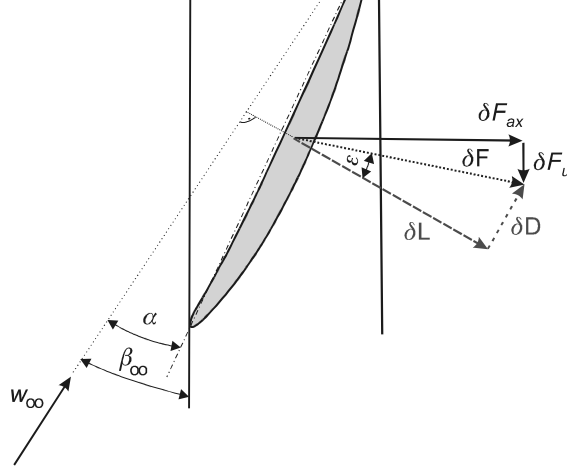


Fig. 4: Blade element with control volume, velocity triangles and exerted angular force δF_u

Eliminating δF_u from eqs. (13) and (17) yields the desired solidity of the blade cascade

$$\sigma \equiv \frac{l}{t} = \frac{4a' \lambda_r}{c_L (1-a) \left(1 - \varepsilon \lambda_r \frac{1+a'}{1-a}\right) \sqrt{\left(\frac{1+a'}{1-a}\right)^2 \lambda_r^2 + 1}}. \quad (18)$$

The circumferential blade spacing for a given number of blades z is:

$$t = \frac{2\pi r}{z}. \quad (19)$$

The overall design power coefficient of the wind turbine is obtained by summing up all elementary strip power coefficients

$$C_P = \eta_{tip} \sum_{\text{all strips}} \eta_{drag} C_{P, BE} \quad (20)$$

weighted with the airfoil drag efficiency

$$\eta_{drag} = \frac{\sin(\beta_\infty - \varepsilon)}{\sin(\beta_\infty)} = 1 - \varepsilon \cot(\beta_\infty) = 1 - \varepsilon \lambda_r \frac{1+a'}{1-a} \quad (21)$$

and an efficiency according to Betz and Prandtl (see Gasch and Twele, 2002) associated with the tip losses

$$\eta_{tip} = \left(1 - 0.92 \sqrt{\lambda_D^2 + \frac{4}{9}}\right)^2. \quad (22)$$

This design method has been encoded in MATLABTM and is our in-house design tool 'dWind'. A further key feature is the integration of the software XFOIL (Drela, 1989) which yields accurately the blade element airfoil lift and drag coefficients as a function of the chosen airfoil, angle of attack and Reynolds number.

DESIGNED ROTOR

Utilizing 'dWind' a small three-bladed wind turbine for a design tip-speed ratio of $\lambda = 7.5$ is designed. The overall sizes are 3 m for the rotor and 0.21 m for the hub diameter, Fig. 5. The blades are fixed pitch and made up of Somers (Somers, 2005) airfoil sections. Lift and drag of the airfoil sections were obtained from XFOIL (Drela, 2001) which uses a linear-vorticity second order accurate panel method for the inviscid analysis. The panel method is coupled with an integral boundary layer method and an approximate e^n -type transition amplification formulation (Mueller, 2001). The ambient disturbance level in which the airfoils operates is characterized in XFOIL by 'NCrit' which was set to the default value 9. Tab. 1 summarizes more key parameters of the turbine.

Tab. 1: Characteristic parameters of the investigated small wind turbine

Airfoil section	S835 for $r/r_{tip} < 0.4$	Design angle of attack α (at all blade sections)	5°
	S833 for r/r_{tip} 0.4 to 0.75		
	S834 for $r/r_{tip} > 0.75$		
Design wind speed c_0	6 m/s	Tip diameter	3 m

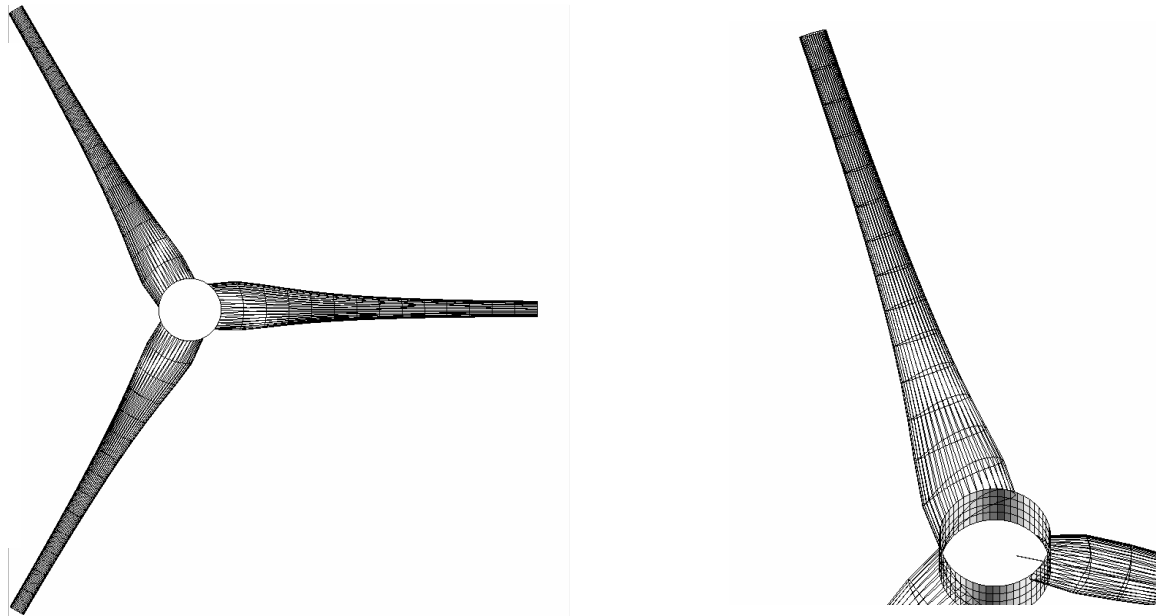


Fig. 5: Rotor and blade of the 3 m wind turbine as obtained by the design software 'dWind'

Because of anticipated structural constraints the blade was modified in the hub region up to $r/r_{tip} = 0.27$, resulting in the fact that the local flow field values of the lower blade part are not comparable to the values predicted by 'dWind'. Furthermore, for a reduction of vortex shedding off from the tip, the tip shape was modified by rounding the leading edge corner at the blade tip (Gyatt and Lissaman, 1985), Fig. 6.

CFD ANALYSIS

Computational domain and boundary conditions

The numerical domain extends four times the rotor radius in upstream and radial direction from the rotor plane and 12 times the radius downstream of the rotor plane, Fig. 6. The turbine symmetry enables the simulation of only one-third of the annulus to save computational costs. Consequently periodic boundary conditions were imposed in the circumferential direction. A velocity inlet was imposed at the upstream boundary with a consistent turbulence intensity of 5% which was assumed to be nearly consistent with 'NCrit' = 9 in XFOIL. The outlet boundary condition consists of an area averaged static pressure ($p_{ave} = p_a$).

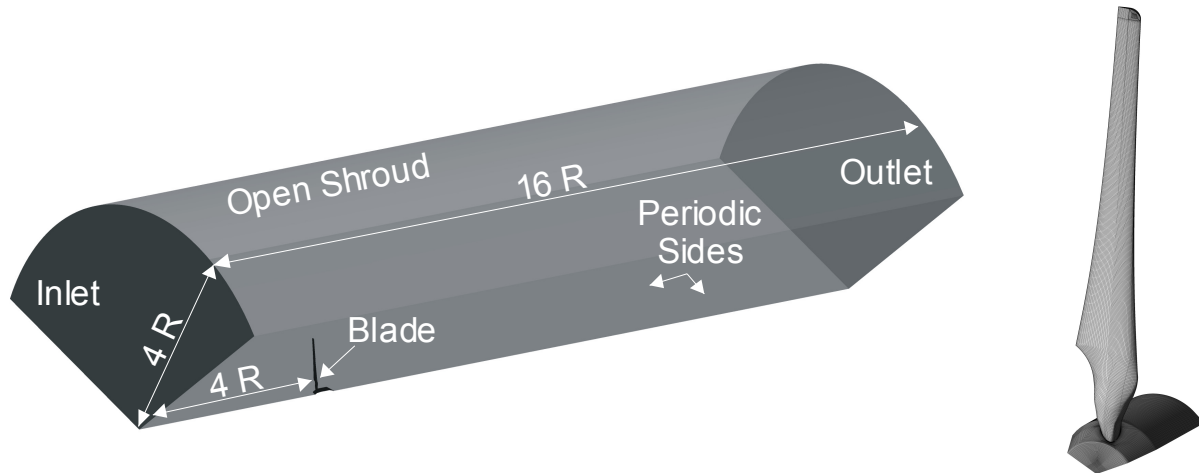


Fig. 6: Left: Computational domain; right: Simulated blade and hub with computational mesh

Numerical scheme and turbulence models

The steady, incompressible, three-dimensional RANS equations are solved in a single rotating reference frame with the commercial 3D Navier-Stokes code ANSYS FLUENT™. For turbulence modeling we used the standard fully turbulent $k\text{-}\omega\text{-SST}$ turbulence model (Menter, 1994) with the default enhanced wall treatment of ANSYS FLUENT™. In order to consider the transitional process taking place on the airfoil surface, we additionally used a laminar/turbulent transition model in ANSYS FLUENT™. Here the $k\text{-}\omega\text{-SST}$ transport equations are combined with an empirical correlation (Menter et al., 2004, Langtry, 2006): Two additional transport equations are implemented, one for the intermittency factor γ and one for the transition onset criterion in terms of the momentum thickness Reynolds number. An empirical correlation describes the difference between a critical Reynolds number, where the intermittency starts to increase and the model is activated, and the transition Reynolds number (ANSYS Inc., 2010). The model constants used by ANSYS FLUENT™ are predominantly taken from Menter et al. (2004).

Numerical grid

While the block-structured numerical grid for the $k\text{-}\omega\text{-SST}$ case consists of 10 million nodes, the transition SST model requires a finer wall resolution which led to a total grid size of more than 18 million nodes. Along the blade span 550 and in chordwise direction 72 non-uniformly spaced nodes were used. This corresponds to a maximum spatial resolution of less than 3 mm. For the $k\text{-}\omega\text{-SST}$ simulation, the maximum value of the dimensionless wall distance y^+ for the first node adjacent to the blade surface was $y_{max}^+ < 30$, whereas the area averaged value y_{ave}^+ at the blade was about 7. The increased wall resolution for the transition SST simulations led to y_{max}^+ values of less than 5 and a blade average below 1.5. Furthermore, common grid quality criteria were considered; for instance the grid angles were all above 25° . However, due to the high wall resolution and the limited node numbers, the aspect ratios for the transitional case were, with maximum values of about 170, quite high. For both cases a convergence criteria of $1 \cdot 10^{-6}$ was reached and integral values were constant over numerous iterations.

Evaluation of the velocity components

The velocity components required for the calculation of the induction factors are evaluated in a reference plane one chord length (at $r/r_{tip} = 0.27$) downstream of the trailing edge. This position of the reference plane was chosen as a good compromise between the very near wake region with the velocities not levelled out at all and the far wake where the stream tube has widened too much. The radial distribution of the relevant flow variables was evaluated by circumferential averaging.

RESULTS

Figs. 7 a) - c) compare the pressure distribution evaluated from the CFD calculations with XFOIL results provided by 'dWind' for an appropriate Reynolds number and basic profile (S834, S833 and S835). The local Reynolds number is based on the corresponding radial chord length l_r and the relative velocity w_l (instead of w_∞)

$$Re_r = w_l l_r / \nu. \quad (23)$$

The pressure-coefficient c_p is defined with the dynamic pressure $p_{dyn,1}$ at the rotor entrance plane as

$$c_p = \frac{p - p_0}{p_{dyn,1}} = \frac{p - p_0}{\rho/2 w_1^2}. \quad (24)$$

The c_p curves of both numerical models fit quite well to the XFOIL predictions. Overall, the transitional case predicts a slightly higher pressure level, in the midspan region even higher than XFOIL. Tab. 2 shows as an example a comparison of the lift coefficient at $r/r_{tip} = 0.9$ for XFOIL, the CFD simulations and 2D experimental wind tunnel data collected by Selig and McGranahan (2003) for the S834 profile. Here the $k-\omega$ -SST model fits quite well to the experimental results while the transition SST model and XFOIL predict a higher lift.

The transitional process, which is taken into account by XFOIL and therefore by our design code 'dWind', is characterized by the bends in the XFOIL pressure distribution. Probably the wall shear stress coefficient presented in Fig. 7 d) shows the transitional process more clearly. Here the XFOIL predictions and the transition SST model correspond quite well. The friction coefficient c_F is calculated with the wall shear stress τ as

$$c_F = \tau / p_{dyn,1}. \quad (25)$$

Tab. 2: Comparison of the sectional lift coefficient

		XFOIL	RANS-prediction		Selig and McGranahan (2003) (clean surface)
			$k-\omega$ -SST	Transition SST	
α	[°]	5	5	5	5.16
Re	[-]	201.388	201.388	201.388	199.991
c_L	[-]	0.85	0.755	0.835	0.766

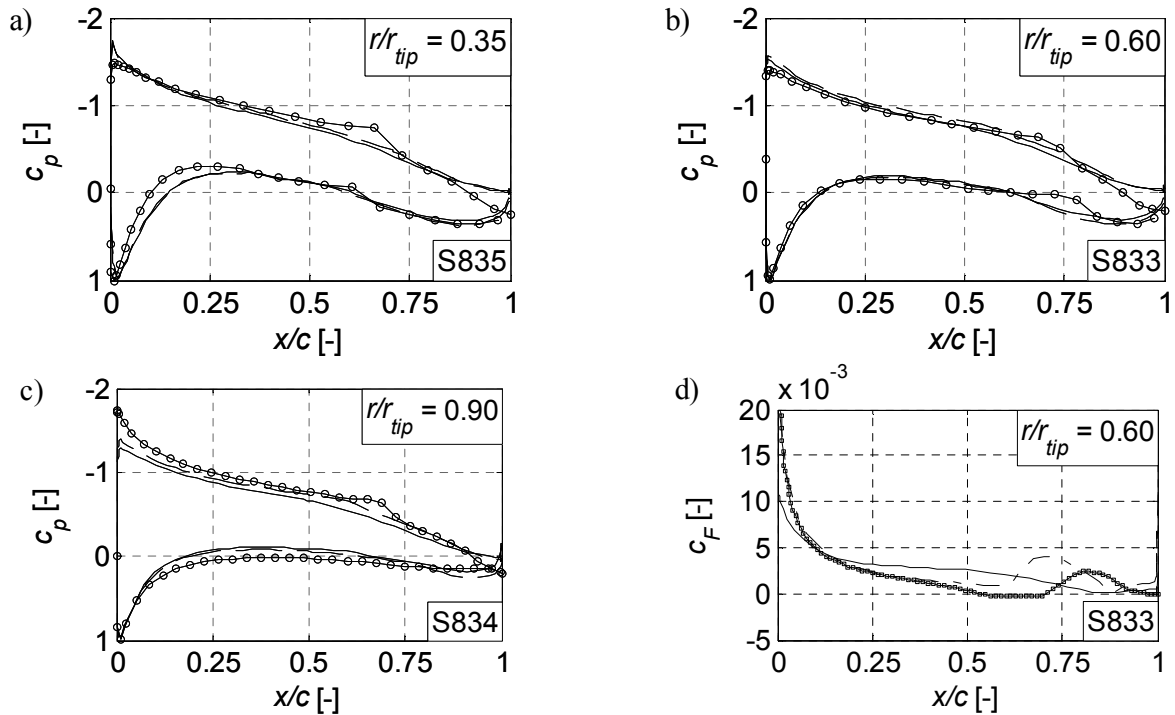


Fig. 7: a) – c) Comparison of c_p at three radial positions; d) Wall shear stress on suction side; solid line: $k-\omega$ -SST model; dashed line: transition SST model; dotted line: XFOIL results

Fig. 8 shows the spanwise distribution of the axial and tangential induction factors a and a' , and the strip power coefficient $C_{P,BE}$. While these quantities are readily available in 'dWind', from the numerically obtained flow field data a has been evaluated according to eq. (1a) with c_{m2} , a' according to eq. (2) with c_{u2} , and $C_{P,BE}$ via eqs. (3), (10), (11) and (12). As aforementioned the results from CFD and the analytical results are only comparable in the outer 73% of the rotor. The agreement between the analytical and numerical data is quite satisfying in the mid span region. While the $k-\omega$ -SST model predicts a slightly lower a , the transition SST model predicts a higher a with increasing radius compared to 'dWind'. In the tip region c_{m2} shows a sharp increase which leads to a decreased a and thus a decrease of $C_{P,BE}$. This trend is consistent with the lower pressure distribution shown in Fig. 7 c). The authors assume that this drop is due to tip effects which are taken into account by 'dWind' only by the global tip loss efficiency η_{tip} while the CFD simulations are 3D.

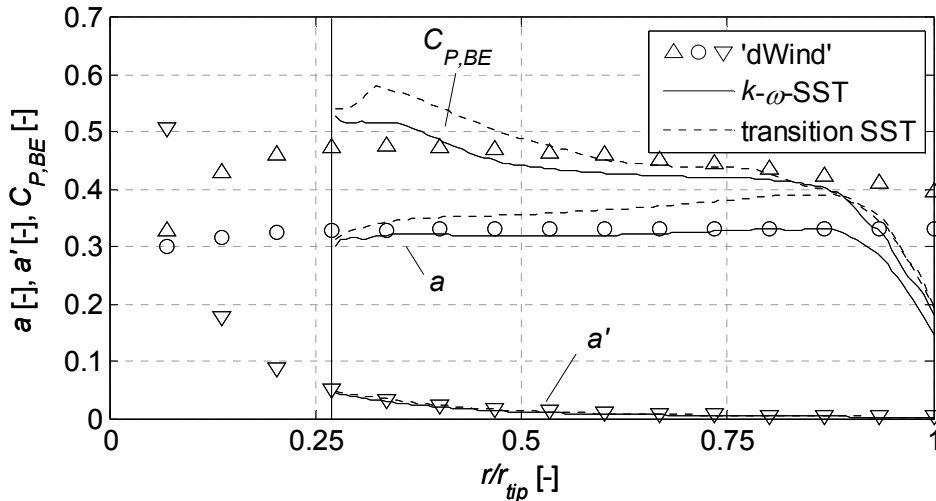


Fig. 8: Design and numerically obtained induction factors and local power coefficient

In Tab. 3 the main performance parameters of the turbine predicted by 'dWind' and calculated from the CFD simulations are listed. On the whole, the agreement between the analytical results and the CFD predicted values is quite satisfying, in particular taking the mentioned modifications in the blade hub and tip region into account.

Tab. 3: Performance parameters at design point for the 3m diameter turbine

		Analytical design (‘dWind’)	RANS-prediction	
			$k-\omega$ -SST	Transition SST
Overall efficiency η (airfoil drag and tip losses)	[%]	76.7	71.3	84.2
Overall power coefficient C_P	[-]	0.44	0.413	0.487
Power output	[W]	431.9	401.5	474.2

CONCLUSIONS

The blade geometry investigated here was designed based on XFOIL (Drela, 1989) as airfoil performance predictor. The agreement between analytical results and CFD predicted values is quite satisfying. However the study shows that the choice of the turbulence model affects the simulated performance of the blade fundamentally.

Comparing the spanwise pressure distributions on selected blade elements as predicted by XFOIL and the $k-\omega$ -SST turbulence model reveal the expected differences: XFOIL clearly shows the transition points, whereas this turbulence model assumes a fully turbulent flow. None the less, the spanwise flow velocities (in terms of a and a') compare quite well while the overall performance parameters of the turbine such as power output and efficiency are slightly lower.

In a second step we took the transitional process on the blades into account by a RANS transition SST model. The overall tendency is that the spanwise pressure distributions agree slightly bet-

ter to the XFOIL results while the spanwise flow velocities as well as the overall parameters are higher compared to the $k-\omega$ -SST model and the values anticipated during design. The better performance is mainly attributed to a smaller profile drag and a simultaneously increased lift, a trend which has also been reported e.g. by Laursen et al. (2007).

Regarding the observed differences one has to keep in mind that 'dWind' is a purely 2D code that completely neglects geometrical features of the blade (hub, tip) and the blade rotation (3D effects). Hence, further analysis is required. For that, we currently build the turbine including instrumentation for collecting experimental data.

ACKNOWLEDGEMENT

Part of the work was done during a sabbatical leave of the coauthor at the Pennsylvania State University (PSU), USA, supported by the Fulbright Commission.

REFERENCES

- ANSYS, Inc. (2010): *ANSYS FLUENT-Theory Guide*, Release 13.0.
- Brouchaert, J.-F. (2007): *Wind Turbine Aerodynamics: A State-of-the-Art*. Lecture Series 2007-5, von Karman Institute for Fluid Dynamics, Belgium
- Burton, T., Sharpe, D., Jenkins, N., Bossanyi, E. (2008): *Wind Energy Handbook*. John Wiley&Sons Ltd.
- Carolus, T., Starzmann, R. (2011): *An aerodynamic design methodology for low pressure axial fans with integrated airfoil polar prediction*. GT2011-45243, Proc. of the ASME Turbo Expo 2011.
- Drela, M.(1989): *XFOIL: An Analysis and Design System for Low Reynolds Number Airfoils*, Conference on Low Reynolds Number Airfoil Aerodynamics, University of Notre Dame.
- Drela, M., Youngren, H. (2001): *XFOIL 6.9 User Primer*, XFOIL documentation, 2001.
- Gasch, R., Twele, J. (2002): *Wind Power Plants*. Solarpraxis AG, Germany.
- Gyatt, G.W., Lissaman, P.B.S. (1985): *Development and Testing of Tip Devices for Horizontal Axis Wind Turbines*, NASA CR 174991, NASA Lewis Research Center.
- Hansen, M.O.L. (2009): *Aerodynamics of Wind Turbines*. earthscan 2009
- Hütter, U.W. (1942): *Beitrag zur Schaffung von Gestaltungsgrundlagen für Windkraftwerke*, Dr. rer. techn. dissertation TH Wien
- Langtry, R.B. (2006): *A Correlation-Based Transition Model using Local Variables for Unstructured Parallelized CFD codes*, Ph.D.-Thesis, University of Stuttgart.
- Laursen, J., Enevoldsen, P., Hjort, S. (2007): *3D CFD Quantification of the Performance of a Multi-Megawatt Wind Turbine*, IOP Publishing, Journal of Physics: Conference Series 75, 012007.
- Manwell, J.F., McWowan, J.G., Rogers, A.L. (2009): *Wind Energy Explained*, John Wiley&Sons Ltd.
- Menter, F.R., Langtry, R.B., Likki, S.R., Suzen, Y.B., Huang, P.G., Volker, S. (2004): *A Correlation based Transition Model using Local Variables - Part 1: Model Formulation*, Journal of Turbomachinery, 128, 413-422, 2004-GT-53452.
- Menter, F. (1994): *Two-Equation Eddy-Viscosity Turbulence Models for Engineering Applications*, AIAA J., 32, 1598-1605.
- Mueller, T.J. (2001): *Fixed and Flapping Wing Aerodynamics for Micro Air Vehicle Applications*. American Institute of Aeronautics and Astronautics, USA.
- Selig, M.S., McGranahan, B.D. (2003): *Wind Tunnel Aerodynamic Test of Six Airfoils for Use on Small Wind Turbines*, Subcontractor Report, NREL/SR-500-34515
- Somers, D.M. (2005): *The S833, S834, and S835 Airfoils*, NREL/SR-500-36340.
- Spera, D. (1998): *Wind Turbine Technology*. ASME Press.